DIRECT ENERGY CONVERSION BY PROTON-CONDUCTING CERAMIC FUEL CELL SUPPLIED WITH CH_4 AND H_2O AT 600-800°C

Satoshi Fukada*, Shigenori Suemori, Ken Onoda
Department of Applied Quantum Physics and Nuclear Engineering, Kyushu University
*Corresponding author: 6-10-1 Hakozaki, Higashi-ku, Fukuoka 812-8581, Japan
Tel +81-92-642-4140, Fax +81-92-642-3800, Email sfukada@nucl.kyushu-u.ac.jp

Abstract

Relations between current density and terminal voltage (I-V curves) of the proton-conducting ceramic of $SrCe_{0.95}Yb_{0.05}O_{3-a}$ were determined for application to a fuel cell working at 600 - 800°C. In a similar way to the introduction of a $H_2 + H_2O$ mixture, its anode supplied with a $CH_4 + H_2O$ mixture worked as a fuel cell efficiently without any external CH_4-to-H_2 reformer. The overall electric resistance for the $CH_4 + H_2O$ supply was larger than that for the $H_2 + H_2O$ supply, because of activation over-potential of the anode electrode. Although a small amount of carbon deposited at a narrow interface between the ceramic and the Ni/SiO_2 electrode, it did not affect cell performance. The overall conductivity was smaller than other fuel-cell systems such as PEM-FC. Application to the recovery of tritium from process streams of a fusion reactor was discussed in terms of the protonic conductivity.

Keywords: proton-conducting ceramic, Sr-Ce-Yb oxide, fuel cell, high temperature, CH_4 steam reforming, internal reform.

1. Introduction

Some doped perovskite-type oxides exhibit proton conduction at higher temperatures. $SrCeO_3$- or $CaZrO_3$-based ceramics demonstrated higher proton-conducting performance at 600°C to 1 000°C [1]. Therefore, application to a hydrogen pump, a hydrogen sensor and a hydrogen (or tritium) purifier operated at 600-800°C is expected in the nuclear engineering field, especially in the tritium recovery process of fusion reactors [2-4]. In order to apply proton-conducting ceramics to produce H_2 and electricity for the effective use of nuclear heat as well as to recover tritium from gas streams in fusion reactors, combining steam-reforming reaction of CH_4 on a Ni catalyst with a proton-conducting ceramic fuel cell was studied experimentally. Especially we focused on mass and charge transfer in a $SrCeO_3$-based proton-conducting ceramic with internal reformation on a Ni electrode under the supply of $CH_4 + H_2O$. The oxide used in the present experiment was $SrCe_{0.95}Yb_{0.05}O_{3-a}$, and the electrodes were composed of a Ni wire mesh and Ni-SiO_2 paste comprising Ni and SiO2 fine particles and a vaporable paste. The cell system was described by $CH_4+H_2O|Ni|SrCe_{0.95}Yb_{0.05}O_{3-a}|NiO|O_2+H_2O$. Several I-V characteristic curves (i.e., electric current density, I, versus cell potential, V) were determined for different H_2O/CH_4 concentration ratios in the temperature range of 600 to 800°C. A thermodynamic electromotive force, E_0, and an overall electric conductivity, σ, were determined from the interrupt on the y-axis of an I-V curve and its slope, respectively. These results were compared with our previous results of the direct and alternating current methods [4,5]. They were determined under the condition where a similar cell system composed of $SrCe_{0.95}Yb_{0.05}O_{3-a}$ and porous Ni/SiO_2 electrodes was supplied with a mixture of $H_2 + H_2O$ in the anode and with a mixture of $O_2 + H_2O$ in the cathode. We observed surfaces in/on the porous anode electrode using a SEM (Scanning Electron Microscope) and an EDX (Energy Dispersive X-ray spectroscopy), and we investigated whether or not carbon deposited in/on the porous Ni/SiO_2 electrode.

Figure 1. Experimental apparatus of a fuel

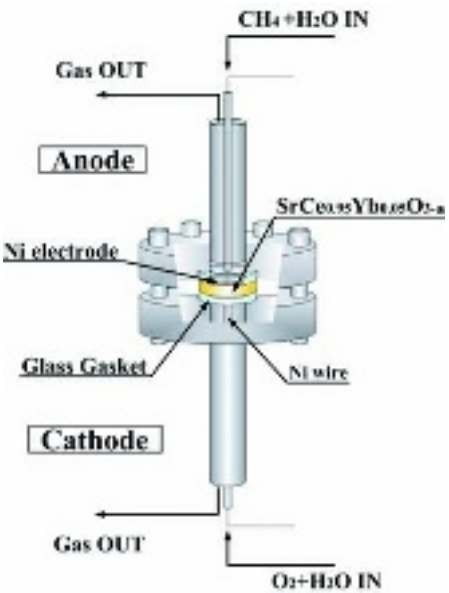

2. Experimental

Figure 1 shows a schematic illustration of the fuel-cell system used in the present study. Ni-SiO_2 paste (Aremco Corp. Pyro-Duct 598) was painted on both surfaces of a $SrCe_{0.95}Yb_{0.05}O_{3-a}$ ceramic pellet with Ni wire mesh. The surface area and thickness of the ceramic pellet was 1.77 cm^2 and 3.5 mm. The ceramic was calcinated in an electric heater at 1 000°C for several hours.

Figure 2. SEM photo of NiO/SiO_2 electrode

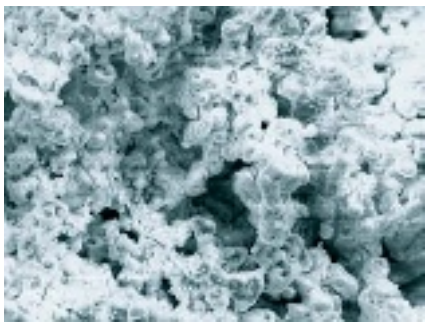

Figure 2 shows a SEM photo of a porous NiO/SiO_2 electrode. The Ni/SiO_2 electrode in the anode was reduced under H2 atmosphere at 800°C for several hours. Figure 3 shows a SEM photo of the $SrCe_{0.95}Yb_{0.05}O_{3-a}$ electrolyte. A structure of multi-crystal ceramic was observed in this photo.

Figure 3. SEM photo of $SrCe_{0.95}Yb_{0.05}O_{3-a}$

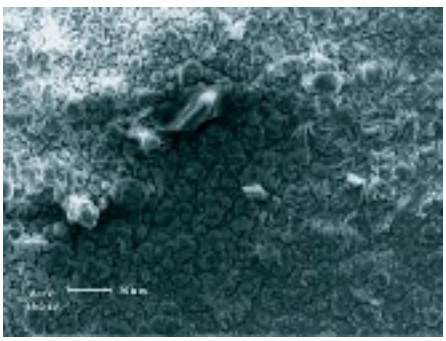

The ceramic pellet with the porous Ni/SiO_2 electrodes was placed in a 316 stainless-steel holder. A glass gasket was used in order to eliminate gas leak through interfaces between the anode and cathode. The anode was supplied with a gas mixture of $H_2 + H_2O$ or $CH_4 + H_2O$. The H_2 concentration was 20%. The CH_4 concentration was 10%. Results for other H_2 or CH_4 concentrations were reported elsewhere [4,5]. H_2O was added to the CH_4 or H_2 gas flow by a bubbler immersed in a constant temperature bath. The cathode was supplied with a mixture of O_2 and H_2O. The H_2O concentration in the cathode was 20%. The concentrations of H_2, O_2, CH_4, CO, CO_2 and other hydrocarbons at the outlets of the anode and cathode were detected by gas chromatography. The H_2O concentration was measured by a dew-point meter. The gas flow rate was controlled to a constant flow rate by mass-flow regulators. The fuel-cell holder was placed in an electric furnace controlled to a constant temperature. Temperature was measured by C-A thermocouples. I-V curves were determined by a two-terminal direct-current method.

3. Results and Discussion

(1) I-V curves

Figures 4 and 5 show typical I-V curves for the Sr-Ce-Yb fuel-cell system. The former figure shows results for different temperatures and the latter does those for different input CH_4/H_2O ratios. As seen in the two figures, the whole I-V curves were correlated to the following relation:

$$V = E_0 - Id/\sigma \qquad (1)$$

Figure 4. I-V curves for $CH_4+H_2O|Ni|SrCe_{0.95}YbO_{3-a}|NiO|O_2+H_2O$ cell

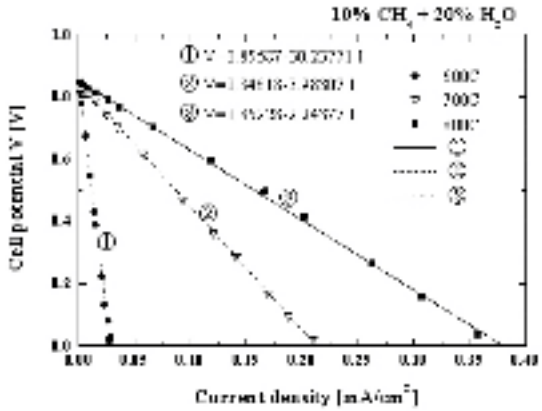

Here, V and E_0 are cell potentials or terminal voltage at arbitral current density I and I = 0. Usually, E_0 is called a thermodynamic electromotive force, EMF. The notations of A and δ are a surface area and thickness of the ceramic electrolyte, and s is an electric conductivity. Since measurement was carried out by a direct current method, the s value corresponded to an overall one including the contributions of anode and cathode polarities as well as the protonic conductivity of ceramic electrolyte. The dependence of E_0 on temperature was very small and almost independent of it. On the other hand, the E_0 values slightly depended on the input CH_4/H_2O ratio.

Figure 5. I-V curves for $CH_4+H_2O|Ni|SrCe_{0.95}YbO_{3-a}|NiO|O_2+H_2O$ cell

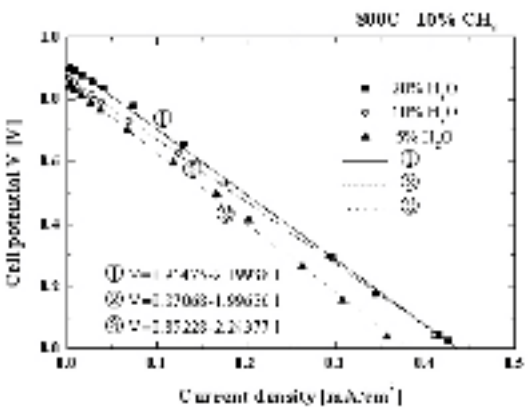

(2) Correlations of E_0 and σ

It was found that the system could work well even without any external CH_4-to-H_2 reformer. Figure 6 shows a relation of E_0 and the partial pressure of H_2O, pH_2O, supplied to the anode. As seen in the figure, E_0 (on the left-hand-side axis) slightly increased with an increase in pH_2O. This is because the steam-reforming reaction proceeded more with elevating temperature. This increase was attributable to a difference in the H_2 partial pressure, pH_2, on the anode electrode. When a CH_4 and H_2O mixture was introduced into the anode, the following CH_4 steam-reforming reaction occurred as well as other by-product reactions [6,7].

$$CH_4 + H_2O = CO + 3H_2 + \Delta H_{CH4\text{-}H2} \qquad (2)$$

The E0 values determined were compared with the following Nernst equation [8].

$$E_0 = -\frac{\Delta G_{H_2O}}{2F} - \frac{R_g T}{2F} \ln\left(\frac{p_{H_2O,cathode}}{p_{H_2,anode}\, p_{O_2,cathode}^{0.5}}\right) \qquad (3)$$

Here, ΔG_{H2O} is a Gibbs free-energy change of the reaction of $H_2 + (1/2)O_2 = H_2O + \Delta H_{H2O}$, and its value was given in the reference [9]. The p_{H2},anode values determined using Eq. (3) were plotted on the right-hand-side axis of Figure 6. Since the residence time of the $CH_4 + H_2O$ gas in the anode was around one second, the exhaust gas was not under equilibrium condition. Since the order of reaction was the first on p_{H2O} [10,11], the partial pressure of H_2 produced in the anode should be in proportion to p_{H2O}. The experimental results also showed a proportional relation between p_{H2O} supplied and p_{H2} produced. Therefore, $p_{H2,\ anode}$ was deeply related with the rate of the steam-reforming reaction of Eq. (2). This will be investigated also in the following discussion on σ.

Figure 6. Relation of EMF and p_{H2} versus p_{H2O}

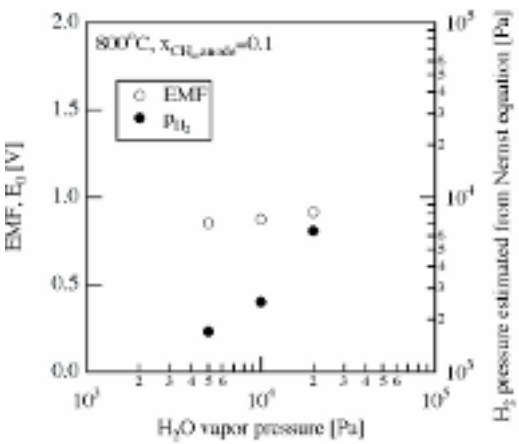

Figure 7 shows a comparison of σ between the $CH_4 + H_2O$ and $H_2 + H_2O$ supplies. As seen in the figure, σ for the $CH_4 + H_2O$ supply was much smaller than that for the $H_2 + H_2O$ one. The ratio became over one-tenth, and the σ values for the $CH_4 + H_2O$ supply were independent of p_{H2O}. Referring to the discussion in our previous paper [4], where complex impedance plots were obtained in the system of a $SrCe_{0.95}Yb_{0.05}O_{3-a}$ fuel cell supplied with $H_2 + H_2O$ mixtures, the rate-determining step of the overall charge transfer was H^+ diffusion in the ceramic electrolyte. Therefore, a decrease in σ for the $CH_4 + H_2O$ supply was not caused by the H^+ conduction in the ceramic electrolyte. This is because the cathode was under the same condition between the $H_2 + H_2O$ and $CH_4 + H_2O$ supplies. The second contribution

was the oxidation reaction of H_2 in/on the cathode. However, it could not be also explained by the same reason. Therefore, the rate-determining step of the charge transfer for the $CH_4 + H_2O$ supply should be related to the steam-reforming reaction of CH_4 on the anode electrode.

Figure 7. Comparaison of conductivity between CH_4+H_2O and H_2-H_2O supplies

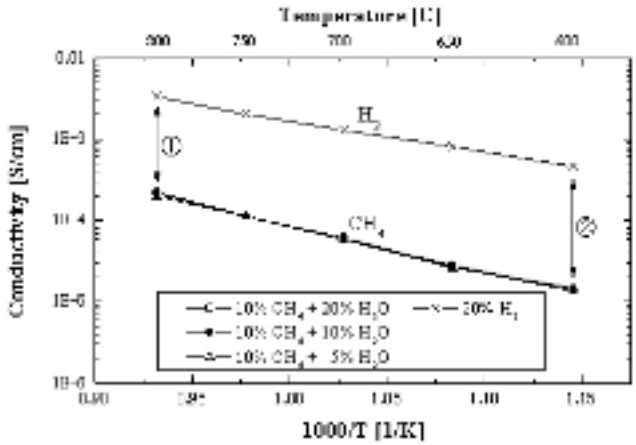

Figure 8. Mass and charge transfer on proton-conducting ceramics fuel cell

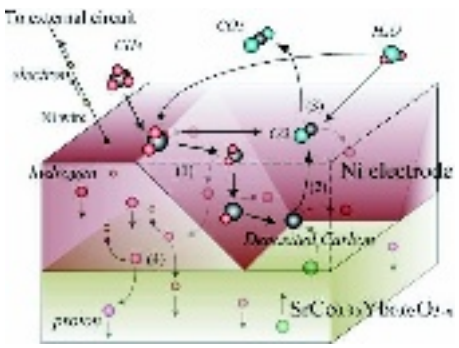

Figure 8 shows a schematic illustration of the anode reaction in the present proton-conducting ceramic fuel-cell system. In the anode, the following reactions may occur simultaneously:

(i) convection of CH_4 and H_2O in the anode,

(ii) CH_4 and H_2O reaction on/in the porous Ni/SiO_2 electrode,

(iii) CH_4 and H_2O diffusing through the porous Ni/SiO_2 electrode,

(iv) reaction product of CO, CO_2 and so on diffusing in a counter-current way,

(v) decomposition to H atom,

(vi) H_2 or H diffusion in the porous Ni/SiO_2 electrode,

(vii) H+ diffusion through the ceramic electrolyte.

The activation energy of σ was 106 kJ/mol for the $CH_4 + H_2O$ supply and 75.6 kJ/mol for the $H_2 + H_2O$ supply. Difference between the two energies was 30 kJ/mol. The value was in close agreement with the activation energy of the reaction-rate constant of Eq. (2) [10]. Therefore, the largest contribution to σ, in other words the rate-determining step, was considered the intrinsic rate of Eq. (2). It was clear that the steam-reforming reaction contributed heavily to the overall conductivity.

(3) Carbon deposition

Figure 9. Profiles of carbon deposition in/on porous Ni electrode

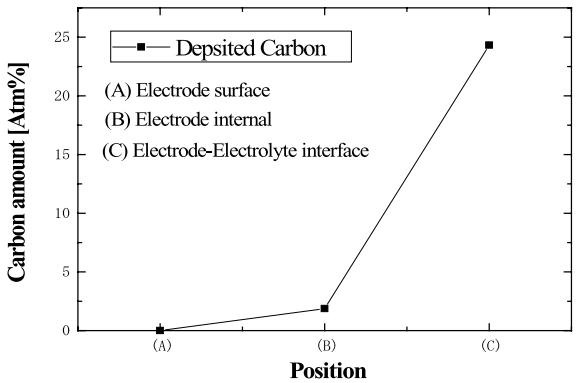

Figure 9 shows the profile of carbon deposition in the porous Ni/SiO_2 electrode determined using SEM-EDX. There was no carbon deposition on its surface. There were also very few carbon depositions in the porous electrode. This was because the following direct decomposition reaction did not occur in/on the porous electrode.

$$CH_4 = C + 2H_2 \qquad (4)$$

The ratio of the CH_4-to-H_2 direct decomposition rate to that of the CH_4 steam-reforming reaction one was not found to be different from location to location in the porous electrode. Therefore, it was considered that the supply of H_2O was sufficient in the present experiment. It was probable that a sufficient amount of CH_4 and H_2O diffused through the porous electrode and arrived at an electrode-electrolyte interface. The direct decomposition reaction as well as the steam-reforming reaction simultaneously occurred at a narrow interface under the condition of the sufficient supply of electric charge to the cathode electrode. As seen in Figure 9, some carbon deposited at the narrow interface between the electrolyte and electrode, This may be because the steam-reforming reaction was slower than the protonic conductivity of electrolyte and, consequently, the direct decomposition of CH_4 provided electron and H+ ion to the interface. Since the carbon deposition was localized at the interface. Therefore, there was no effect on the mass and charge transfer in the present cell system.

The Sr-Ce oxides were stable at 600-800°C when H_2O was added in the streams of anode and cathode. The addition of H_2O was necessary in order to maintain protonic conduction through the ceramic electrolyte [4]. However, it is known that Sr-Ce oxides decomposed to $SrCO_3$ and CeO_2 at high CO_2 atmosphere [12]. Therefore, the use of the Sr-Ce oxide is not proper under the condition of CO_2 atmosphere. In the present study, gas composition detected in the exhaust from the anode was CH_4, H_2, H_2O, and CO. No CO_2 was observed throughout the present study. This may be because the reaction temperature was higher than 600°C, and a sufficient amount of H_2O was supplied to the anode and cathode. There was high possibility of production of CO_2 at lower temperatures of 300-500°C [7]. The use of a compact Ni electrode in place of the porous Ni/SiO_2 electrode may be proper if CO_2 is

generated in the anode. The ceramic electrode with a compact Ni electrode that was electrically deposited will not contact with CO_2 directly. Therefore, there may be no possibility of the decomposition to $SrCO_3$ and CeO_2.

(4) Application of Sr-Ce-Yb oxide to high-temperature system

There are several advantages and disadvantages for the present Sr-Ce-Yb oxide fuel-cell system. The largest advantage is that it can work at 600-800°C, at which the steam-reforming reaction simultaneously occurred. The internal reformation became possible at these temperatures. Therefore, its structure became very simple. Heat to maintain the steam-reforming reaction can be converted to electricity directly because of endothermic reaction of Eq. (2). This thing makes it possible to convert the chemical energy of CH_4 to electricity with a higher efficiency. The Carnot-cycle efficiency can be raised by operation at higher temperatures. Its working temperature is near that of a high-temperature nuclear reactor. Therefore, it may be possible to provide measures to utilise nuclear heat with high efficiency. This thinking is taken into consideration in other countries in different ways. There are applications of some ceramics to high-temperature steam electrolysis with use of nuclear heat, such as Generation IV nuclear energy system [13].

On the other hand, the largest disadvantage is that the protonic resistance of the Sr-Ce-Yb oxide was comparatively larger than that of a polymer-electrolyte-membrane fuel cell (PEM-FC) and was comparable with O^{2-} ion conductivity of an yttria-stabilised zirconia (YSZ). Consequently, as seen in Figs. 4 and 5, the current density through the Sr-Ce-Yb oxide fuel cell was order of mA/cm^2 and was much smaller than that of PEM-FC. This is because a thin ceramic is very difficult to manufacture. The protonic conductivity of the Sr-Ce-Yb oxide itself was around one-tenth smaller than that of PEM. Moreover, the conductivity was order of 10^{-4} S/cm when a CH_4 and H_2O mixture was supplied directly to the cell without external reformer. The overall conductivity became around 10^{-2}-fold less than that of PEM, because the rate-controlling step was in the steam-reforming reaction.

Judging from the data available in the present study, it is difficult to apply the Sr-Ce-Yb oxide (as it is) to the effective use of nuclear reactor heat, where a large amount heat should be converted to electricity. Considering H_2 production rate, the current density of 1 mA/cm^2 corresponds to the H_2 production rate of 1.2×10^{-6} Nm^3/m^2s. Therefore, the surface area of 8.6×10^5 m^2 is necessary for the H_2 production rate of 1 Nm_3/s. This is an unrealistic scale. On the other hand, it is desirable to utilise the proton-conducting ceramic under special or severe conditions, such as hydrogen or tritium pump at higher temperatures. Converting to tritium activity, the current density of 1 mA/cm^2 corresponds to 11 MBq/cm^2s. Since the tritium generation rate in a blanket to maintain 1 GW commercial fusion power reactor is 0.63 TBq/s, the surface area of the Sr-Ce-Yb oxide necessary to extract tritium from $CH_4 - H_2O$ or $H_2 - H_2O$ streams as a tritium pump amounts to 5.7 m^2. It is expected that the tritium pump will be operated at 600-800°C in a blanket tritium recovery system or a tritium purification system in a fusion fuel cycle. This is a realistic scale.

4. Conclusions

The I-V curves for the fuel-cell system composed of a $SrCe_{0.95}Yb_{0.05}O_{3-a}$ ceramic electrolyte and Ni/SiO_2 porous electrodes were determined under the conditions of $CH_4 + H_2O$ and $H_2 + H_2O$ supplies, and the values of E_0 and σ were correlated to a function of temperature and the anode H_2O partial pressure. The E_0 values were consistent with the Nernst equation. It was found that E_0 was a good indication of p_{H2} generated on the anode electrode when the CH_4 and H_2O mixture was introduced into the anode. The σ values determined included the two contributions of the protonic conductivity of the

Sr-Ce-Yb oxide electrolyte and the activation polarity of the steam-reforming reaction on the Ni/SiO2 porous electrode. Because of stable operation of the Sr-Ce-Yb oxide as a fuel cell at 600-800°C, it is expected to utilise the ceramic for tritium pump. The profile of carbon depositions were determined by SEM-EDX, and it was found that carbon depositions by the direct decomposition of CH_4 were localised at a narrow interface between the electrode and electrolyte.

REFERENCES

[1] H. Iwahara, Solid State Ionics, 77 (1995) 289-298.

[2] Y. Kawamura, S. Konishi, M. Nishi, Fus. Sci. Technol., 45 (2004) 33-40.

[3] M. Tanaka, K. Katahira, Y. Asakura, T. Uda, H. Iwahara, I. Yamamoto, J. Nucl. Sci. Technol., 41 (2004) 61-67.

[4] S. Fukada, K. Onoda, S. Suemori, J. Nucl. Sci. Technol., 41 (2005) 1-7.

[5] S. Fukada, S. Suemori, K. Onoda, J. Nucl. Mater., in printing.

[6] S. Fukada, N. Nakamura, J. Monden, M. Nishikawa, J. Nucl. Mater., 329-333 (2004) 1365-1369.

[7] S. Fukada, N. Nakamura, J. Monden, Int. J. Hydrogen Energy, 29 (2004) 619-625.

[8] P. W. Atkins, “Physical chemistry”, Oxford University Press, England, (1990).

[9] O. Kubaschewski, C. E. Alcock, “Metallurgical Thermochemistry, 5th ed.”, New York, Pergamon Press, (1979).

[10] W. Jin, X. Gu, S. Li, P. Huang, N. Xu, J. Shi, Chem. Eng. Sci., 55 (2000) 2671-2625.

[11] I. Alstrup, J. Catalyst, 151 (1995) 216-225.

[12] T. Scherban, A. S. Nowick, Solid State Ionics, 35 (1989) 189-194.

[13] For examples, http://www.futurepundit.com/archives/002495.html

TABLE OF CONTENTS